CONF-890294--1

# ROLE OF ALLOYING ADDITIONS IN THE OXIDATION–SULFIDATION OF Fe–BASE ALLOYS*

K. Natesan and J. H. Park
Materials and Components Technology Division
Argonne National Laboratory
Argonne, IL 60439

CONF-890294--1

DE89 009825

March 1989

**DISCLAIMER**



INVITED PAPER presented at the Symposium on "Corrosion and Particle Erosion at High Temperatures," TMS-AIME, Las Vegas, NV, February 27-March 3, 1989; to be published in symposium proceedings.

*Work supported by the U. S. Department of Energy, Advanced Research and Technology Development Fossil Energy Materials Program, Work Breakdown Structure Element ANL 3(A), under contract W-31-109-Eng-38.

---

# ROLE OF ALLOYING ADDITIONS IN THE OXIDATION–SULFIDATION OF Fe–BASE ALLOYS*

K. Natesan and J. H. Park
Materials and Components Technology Division
Argonne National Laboratory
Argonne, IL 60439

## ABSTRACT

Thermogravimetric studies have been conducted on Fe–25 wt % Cr and Fe-25 wt % Cr–20 wt % Ni model alloys with and without additions of refractory metals such as Nb and Zr. In addition to bulk alloying, specimens of both alloys were prepared with surface implantation of Nb. The alloys with bulk additions of Nb and Zr exhibited $Cr_2O_3$ surface scales upon exposure to air and low–$p_{O_2}$ environments. The oxide grain size was much larger than that observed in the absence of Nb/Zr addition. In the oxygen–sulfur mixed–gas environments, the Nb– and Zr–modified alloys exhibited a barrier layer of an oxide of Nb or Zr at the $Cr_2O_3$/substrate interface; this layer minimizes the outward transport of base–metal elements, thereby extending the time for initiation of breakaway corrosion. Experiments conducted with Nb–implanted binary and ternary alloys showed no effect on the oxidation rate in air and low–$p_{O_2}$ environments; however, the oxide grain size was substantially larger compared to that observed in the absence of implant. The Nb implant resulted in a substantial reduction in the oxidation rate of both alloys when exposed in low– and high–sulfur mixed–gas atmospheres. Information on the morphological features of the scales in these specimens as well as possible reasons for the implant benefit is presented.

## INTRODUCTION

Upon exposure to aggressive gaseous environments at elevated temperatures, structural alloys depend on their ability to form and maintain protective surface oxide scales to minimize the rate of corrosive degradation. In principle, one of three oxides, $Cr_2O_3$, $Al_2O_3$, or $SiO_2$, is the major component of thermally formed scales. In oxygen-sulfur mixed-gas environments, typical of those encountered in coal-gasification and combustion atmospheres,experience shows that a thermodynamically stable protective oxide may not form, owing to the presence of sulfur in the gas phase.[1] In practice, an excess of oxygen above the level defining thermodynamic equilibrium between $Cr_2O_3$ and "CrS" is required to form $Cr_2O_3$ as a continuous surface layer.[2] Furthermore, the effect of lowering the exposure temperature is to increase the threshold $p_{O_2}$ for oxide formation. On the basis of the morphological information developed on a number of commercial engineering alloys, advanced highly alloyed metallic materials, and model alloys exposed to oxygen-sulfur mixed-gas environments it became evident that research is needed to modify the alloys to achieve (a) formation of protective surface oxide scales at lower threshold $p_{O_2}$ levels (than presently feasible) in sulfur containing environments and (b) longer exposure times before the initiation of breakaway corrosion in the alloy. With regard to both these areas, extensive research has been in progress at Argonne National Laboratory. This paper will discuss the role of alloying additions, primarily Nb, to Fe-25 wt % Cr and Fe-25 wt % Cr-20 wt % Ni alloys. Nb additions were made both via bulk alloying and as a surface modification, the details of which are presented in subsequent sections.

## EXPERIMENTAL PROCEDURE

### 1. Bulk Alloying

All alloys used in the present investigation were based on the ternary composition Fe-25 wt % Cr-20 wt % Ni with nominal Zr and Nb contents of 0, 1, 3, and 6 wt %. After casting into ingot form, each alloy was rolled to a thickness of 1.25 mm and heat treated at 1100°C to produce homogeneous metallographic structures. Intermetallic compounds were present in the Zr- and Nb-modified alloys owing to the very low limits of solubility of Zr and Nb in the Fe-Cr-Ni alloy matrices. The residual level of Zr or Nb in the alloy matrix was below the limit of detection (~0.05 wt % ) of an x-ray energy dispersive analyzer. At a 3 wt % level of Zr or Nb, the intermetallic particles had the compositions $(Fe_{1.64}Cr_{0.75}Ni_{0.55})Nb$ in the Nb-modified alloy and $(Ni_{3.27}Fe_{1.30}Cr_{0.43})Zr$ in the Zr-modified alloy.[3] The low level of Cr in the intermetallics resulted in a higher concentration of the intermetallic phases at the temperatures of annealing and their fine distribution (5-10 μm particles with 10-20 μm spacing) restricted grain growth and yielded a grain size of 12 μm compared with 50 μm in the pure ternary alloy. Specimens of 13 x 10 x 0.8 mm were ground on SiC paper to a final surface finish of 600 grit, cleaned in ethanol and acetone, and dried prior to testing.

## 2. Ion Implantation

Base alloys of two compositions, namely Fe-25 wt % Cr and Fe-25 wt % Cr-20 wt % Ni, were used in the ion implantation studies. The base alloys were obtained from Carpenter Technology Corporation. The alloys were prepared by vacuum Induction Melting followed by Electro-slag Refining to minimize undesirable contaminants. After melting, the alloys were cast into ~82 mm round ingots. The alloy compositions are given in Table I. After refining, the alloys were cast into ~147 mm round ingots. These ingots were soaked for two hours at ~1176°C for the Fe-Cr-Ni alloy and at 1065°C for the Fe-Cr alloy, and forged into rods of ~57 mm square cross section. The forged alloys were cut and reheated to the soaking

temperature for 0.5 h, hot rolled into rods (~25 mm square cross section) and slowly cooled to room temperature. The rods were subsequently hot rolled into sheets and were given a final anneal at 1050°C for ~1 h. Specimens of 11 x 11 x 0.7 mm were prepared and given a final 1 μm diamond polish.

The finely polished specimens of both base alloys were used for implantation of niobium. The implantation was performed at Implant Sciences. An implant energy of 182 keV and a dose level of $4 \times 10^{16}$ ions/$cm^2$ were used. Implant depth profile calculations were made assuming several different values for the sputtering coefficient and the calculated profiles are shown in Fig. 1. Auger electron spectroscopy was used to determine the depth profiles in the implanted specimens as well those exposed in various gaseous environments. The results will be presented in the subsequent sections.

## 3. Oxidation/sulfidation Experiments

Thermogravimetric (TGA) tests were conducted using an electrobalance, made by CAHN Instruments, Inc., that had a sample capacity of 2.5 g with a sensitivity of 0.1 μg. The furnace consisted of three-zone Kanthal heating elements with a temperature capability of 1100°C in continuous operation. The test specimens were suspended from the balance with an ~200 μm diameter platinum wire. The tests were started at room temperature and purging the system with the appropriate reaction gas mixture. The specimen was heated in the reaction gas to the desired test temperature. The heating time was normally less than 1200 s. Four different reaction gas mixtures were used in the experiments, namely, high-purity air, a 1 vol % CO-$CO_2$ gas depicting a low $p_{O_2}$ environment, and two other reaction gases containing of CO, $CO_2$, $H_2$, and $H_2S$. The relative flow rates of the different gases were adjusted to achieve two different sulfur levels in the reaction gas. Table II lists

the calculated oxygen and sulfur partial pressures established by different reaction gas mixtures. Upon completion of the test, the furnace was opened and the specimen was cooled rapidly in the reaction gas environment. The cooling time to reach ~100 C was generally less than 600 s.

Subsequent to thermogravimetric tests, the corrosion product scales were analyzed using several electron-optical techniques. A scanning electron microscope equipped with an energy dispersive x-ray analyzer was used to examine the exposed surfaces and cross sections. Auger Electron Spectroscopy was used to determine the depth profiles of several exposed specimens, especially those with niobium implantation.

## RESULTS AND DISCUSSION

### 1. Bulk Alloying

Over the past few years, extensive work has been conducted to evaluate the role of bulk additions of Nb and Zr in the improvements of corrosion resistance of Fe-Cr-Ni alloys exposed to oxygen-sulfur mixed gas environments. Both Zr and Nb promote the formation and maintenance of chromium-rich oxide scales.[4,5] The results obtained on these modified alloys have been extensively published elsewhere. The studies, in general, have shown that the alloys with 3 wt % addition of Zr or Nb exhibit protective oxide scales, while the commercial Type 310 stainless steel exposed to the same oxygen-sulfur atmosphere underwent breakaway corrosion (see Fig. 2). The kinetics of scaling, given by the slope of the weight change versus time plot indicates a substantial improvement due to Zr and Nb additions. Furthermore, earlier work showed that alloying with 3 wt % Zr or Nb reduces the level of excess oxygen required for surface oxide scale formation by

approximately one order and half an order of magnitude at 875 and 1000°C, respectively.

The bulk alloying additions also resulted in extending the time for onset of breakaway corrosion.[3] Figure 3 shows a comparison of typical weight-change data developed at 875 C for pure Fe-25 wt%Cr-20 wt%Ni alloys with and without additions of Zr and Nb. A detailed analysis of scales developed in these studies have shown that refractory metal additions lead to a Zr- or Nb-rich interfacial layer (see Figure 4) at the $Cr_2O_3$/substrate interface, thereby minimizing the flux of base metal cations such as Fe and Ni from the substrate through the scale to the gas/scale interface. However, the beneficial effects of refractory metal additions to the bulk alloy have been observed at elevated temperatures in the range 875 to 1000 C and the exposure times needed to achieve similar benefits at lower temperatures (500 to 700 C) may be substantial. An alternative approach of modifying the surface via Nb implantation was undertaken to improve the oxidation-sulfidation resistance of the alloys at lower temperatures.

## 2. Ion Implantation

### *a. Air Oxidation*

Figure 5 shows the AES signals as a function of sputtering time (which is proportional to the specimen depth) for specimens in the as-implanted condition and after 170 h exposure to air at 700°C. The Nb concentration in the as-implanted specimen has a peak at sputtering time of ~10 min and Nb seems to diffuse into the alloy with exposure, as evidenced by the Nb depth profiles in exposed specimens Contrary to the (Fe,Cr) oxide scale developed in an air–exposed ternary Fe-Cr-Ni alloy, the oxide scale in the implanted alloy was predominantly Cr oxide with very little iron. The absence of iron in the oxide scale indicates that the Nb implant

stabilizes the Cr oxide and also minimizes the transport of iron from the substrate. Nb additions can lead to grain refinement in the base alloy as well as lead to an effective increase in chromium concentration in the alloy. Such an influence of Nb has been reported in our earlier work conducted with bulk additions of Nb to Fe-Cr-Ni alloy.[3,5]

Figure 6 shows the SEM photographs of surfaces of Fe-25 wt % Cr alloy in the as-implanted condition and after 170 h of exposure in air at 700°C. The scale was predominantly Cr oxide. The physical size of the globular oxide particles was ~1 to 2 μm which are significantly larger than the value of 0.1 to 0.3 μm observed in the absence of implantation. Such an increase in grain size of the oxide in alloys with refractory metal additions has been reported in our earlier studies.[6]

Figure 7 shows the TGA test data for Fe-25 wt % Cr and Fe-25 wt % Cr-20 wt % Ni alloys with and without Nb implant in air at 700°C. The absolute values of weight changes are extremely small in all cases and Nb implant seems to have very little effect, if any, on the oxidation rate. However, an analysis of surfaces of oxidized samples (see Fig. 8) shows that the oxide grain size is larger with Nb implant than that for the pure binary alloy. Even in the case of the ternary Fe-Cr-Ni alloy, the oxide grain size is somewhat larger even though the Nb implanted specimen was exposed only half as long as the pure ternary alloy.

*b). Low-$p_{O_2}$ Oxidation*

Since the oxygen-sulfur mixed gas environments in coal-gasification systems involve $p_{O_2}$ values that are orders of magnitude lower than that of air, TGA experiments were conducted to examine the oxidation behavior of Nb–implanted specimens under low $p_{O_2}$ conditions. Figure 9 shows the weight–change curves for specimens of Fe-25 wt % Cr and Fe-25 wt % Cr-20 wt % Ni with and

without Nb implant exposed to 1 vol % $CO-CO_2$ gas mixture at 700°C. The results show that the weight changes are comparable to those observed in air-exposed specimens. As before, the Nb implant had very little effect, if any, on the oxidation rate. The oxide scales were predominantly Cr oxide with almost no iron in them. Figure 10 shows the SEM photographs of surfaces of the two alloys with and without Nb implant after exposure to low $p_{O_2}$ at 700°C. The oxide scales in the Fe-Cr-Ni alloy were extremely thin as evidenced by the polishing lines; however, the oxide grain size in the Nb implanted specimen is somewhat larger than that without implant even though the exposure time for the implanted alloy was only a third of that without implant. On the other hand, the Fe-25 wt % Cr alloy exhibited a much denser and fine grained oxide in the implanted condition than without implant. It is not clear whether this difference in morphology between the binary and ternary alloys translates to a difference in the sulfur resistance of the scales.

*c. Exposure in Oxygen-Sulfur Mixed Gas*

Two different oxygen-sulfur mixed gas mixtures (see Table II) were selected for the exposure of Nb implanted specimens. Figure 11 shows the TGA data for Fe-25 wt % Cr and Fe-25 wt%Cr-20 wt%Ni alloys with and without Nb implant after exposure to low sulfur mixed gas environment. The results clearly indicate a substantial reduction in the oxidation rate of the implanted alloys of both base compositions. Figure 12 shows the SEM photographs of the surface morphology of the oxidized alloys. The alloys without Nb implant exhibited sulfide mode of attack while those with the implant showed an oxide mode of interaction. The oxide scale thicknesses in the implanted specimens were comparable to those observed in sulfur-free environments. The oxide scales were predominantly Cr oxide with very little iron, as was observed in studies conducted in sulfur-free atmospheres. Figure 13 shows the SEM photographs of the cross sections of the oxidized alloys. The scale

thicknesses in alloys without implant ranged between 20-25 μm while those in implanted alloys were in the range 1-2 μm.

Figure 14 shows the TGA data for the two alloys with and without Nb implant after exposure to high-sulfur mixed gas at 700°C. Again the corrosion rates are substantially lower for Nb–implanted specimens than the base alloys without implant. The absolute rates for the implanted specimens exposed to the high sulfur gas are somewhat higher than those exposed in sulfur-free or low sulfur mixed gas environments. But neither of the implanted alloys undergo breakaway corrosion in the exposure times of the present investigation. Among the two alloys, the Fe-25 wt % Cr composition had a much more beneficial effect due to the implant. Figure 15 shows the surface morphologies of the two alloys with and without implant after exposure to high sulfur environment. It is evident that the alloys without implant and the ternary alloy with implant underwent sulfide mode of attack. The binary alloy with implant exhibited an oxide mode of attack with some particles of sulfide on the surface. Figure 16 shows the cross sections of the two alloys with and without implant after exposure to high sulfur mixed gas. The specimens without implant exhibited scale thicknesses in the range 200-600 μm while those with the implant showed scales of 10-30 μm in thickness.

Extensive AES analysis of exposed specimens showed some differences in scale compositions depending on whether sulfur was present or absent in the exposure atmosphere. For example, the depth profile analysis of the implanted binary alloy and exposed to low-sulfur mixed-gas showed virtually no iron in the chromium oxide scale to a depth of 2 μm. This indicates that the Nb implantation process effectively increases the diffusivity and thermodynamic activity of Cr in the alloy in the implanted region. It is possible that the diffusivity alone can be increased due to the implant damage created by an inert implant, but such a process

will lead to increases in diffusivities of iron as well as chromium. The scale composition results clearly indicate that Nb plays a role in stabilizing the $Cr_2O_3$ scale. Furthermore, there was a complete absence of sulfur in the scale developed under low-sulfur conditions. The Nb implanted binary alloy exposed to high-sulfur environment developed a sulfide scale; however, the scale was predominantly chromium sulfide and iron was virtually absent over a depth of 8 μm in the AES depth profile analysis. The low growth rate of "CrS" coupled with absence of FeS can extend the time for the onset of breakaway corrosion in the alloy.

In addition, the scales in the Fe-25 wt % Cr and Fe-25 wt % Cr-20 wt % Ni alloys were somewhat different, even though both had the same level of implanted Nb. AES depth profile analysis of Nb implanted ternary alloy exposed to air and low-oxygen gas showed predominantly $Cr_2O_3$ scales. The absence of iron, especially in the scale developed in air, indicates that Nb implant stabilizes chromia scale since in the absence of implant the scale will be predominantly ( Fe, Cr) oxide. The implanted ternary alloy developed (Fe, Cr)- and (Fe,Ni)–sulfide scales in low- and high-sulfur exposures, respectively. However, the scale thicknesses in the Nb implanted specimens were about 20 times lower than in the non-implanted specimens (see Fig. 16), the cause of which cannot be explained at with the AES depth profile analysis.

## SUMMARY

Thermogravimetric experiments were conducted on binary Fe-Cr and ternary Fe-Cr-Ni alloys with bulk additions of refractory elements such as Nb and Zr and with implantation of Nb in the surface region. The tests were conduced in four different exposure environments namely, air, low-oxygen gas, and low- and high-

sulfur mixed gases. Several conclusions can be drawn on the role of refractory metal additions in the oxidation/sulfidation behavior of Fe-Cr and Fe-Cr-Ni alloys.

The effects of Nb and Zr additions via bulk alloying are as follows:

1. The threshold oxygen partial pressure for oxide formation is lower by factors of 5 to 10 with additions of 3 wt % Nb or Zr.

2. The additions of Nb and Zr lead to grain refinement in the substrate alloy which can influence the nucleation/growth of the oxide scale, especially in the early stage of oxidation in the mixed-gas atmospheres.

3 The oxide scale thicknesses are substantially lower with the additions of Nb and Zr than without them. The Cr oxide scales exhibit better adherence to the substrate via formation of refractory-metal oxide pegs at the scale/metal interface.

4. The oxide grain sizes is much larger in the Nb- and Zr-modified alloys compared with those in base alloys.

5 The time for the onset of breakaway corrosion, which occurs in oxygen-sulfur mixed-gas atmospheres, is much longer in Nb- and Zr-modified alloys than those for the base alloys. The reason for this time extension is the formation of a barrier layer of refractory metal oxide at the $Cr_2O_3$/substrate interface which minimizes the outward flux of base-metal elements such as Fe and Ni. However, the formation of the barrier layer is favored at higher temperatures in the range 800 to 1000°C.

The effects of Nb addition via implantation are as follows:

1. Nb implantation has very little effect on the oxidation rate of both binary Fe-Cr and ternary Fe-Cr-Ni alloys exposed to air or low-oxygen environments.

2. The oxide grain size in the implanted alloys are much larger than in the base alloys without implant.

3. The oxide layer is predominantly $Cr_2O_3$ in the implanted alloys with virtual absence of Fe in the scale.

4. The implanted alloys exhibited substantial improvement in sulfur resistance in both low- and high-sulfur mixed-gas environments. The implanted binary alloy developed Cr oxide and Cr sulfide scales under low- and high-sulfur mixed-gas exposures, respectively. Iron was virtually absent in the scales in both exposures. The implanted ternary alloy developed (Fe, Cr) sulfide and (Fe,Ni) sulfide under low- and high-sulfur mixed-gas exposures, respectively. However, the scale thicknesses in the implanted alloys were in the range of 10 to 30 μm while those in the base alloys without implant ranged between 200 to 600 μm.

## ACKNOWLEDGMENTS

This work was supported by the U. S. Department of Energy, Advanced Research and Technology Development, Fossil Energy Materials Program [Work Breakdown Structure Element ANL 3(A)], under contract W-31-109-Eng-38. D. L. Rink assisted with the experimental program.

## REFERENCES

1. K. Natesan and M. B. Delaplane, Proc. Symp. on Corrosion-Erosion Behavior of Materials, Fall Mtg. of TMS-AIME, October 1978, K. Natesan, Ed., AIME, New York, p.1 (1980).

2. T. C. Tiearney, Jr. and K. Natesan, Oxid. Metals, 17, 1 (1982).

3. D. J. Baxter and K. Natesan, Oxid. Metals, in press.

4. D. J. Baxter and K. Natesan, Corrosion Science, 26, 153 (1986).

5. D. J. Baxter and K. Natesan, in Proc. Third Berkeley Conf. on Corrosion-Erosion-Wear of Materials at Elevated Temperatures, Berkeley, CA, January 27-29, 1986, Ed. A. V. Levy, NACE, Houston, p.309 (1987).

6. D. J. Baxter and K. Natesan, Oxid. Metals, 24, 331 (1985).

## Figure Captions

Fig. 1. Calculated depth profiles for Nb implantation in Fe-Cr alloys.

Fig. 2. Weight change data for commercial 310 stainless steel and Ti-, Nb-, and Zr-modified Fe-25 wt %C r-20 wt % Ni alloys exposed to a mixed gas environment.

Fig. 3. Thermogravimetric test data for alloys exposed to a mixed gas mixture at 875°C following preoxidation for 72 h at 875°C in an atmosphere with $p_{O_2} = 2*10\text{-}^{14}$ atm.

Fig. 4. (Left) Cross section of a Nb-modified alloy specimen after preoxidation at 1000°C, showing the two-layer oxide scale; (right) Nb x-ray map.

Fig. 5. AES depth profile analysis for Fe-25 wt % Cr alloy in the Nb-implanted condition and after air oxidation for 170 h at 700°C.

Fig. 6. SEM micrographs of surfaces of Fe-25 wt % Cr alloy in the Nb-implanted condition and after air exposure for 170 h at 700°C.

Fig. 7. Weight change data for Fe-25 wt%Cr and Fe-25 wt % Cr-20 wt % Ni alloys with and without Nb implant after air exposure at 700°C.

Fig. 8. SEM micrographs of surfaces of Fe-25 wt%Cr and Fe-25 wt%Cr-20 wt%Ni alloys with and without Nb implant after air exposure at 700 C

Fig. 9. Weight change data for Fe-25 wt % Cr and Fe-25 wt % Cr-20 wt % Ni alloys with and without Nb implant after exposure to a low-oxygen environment at 700 C.

Fig. 10. SEM micrographs of surfaces of Fe-25 wt%Cr and Fe-25 wt%Cr-20 wt%Ni alloys with and without Nb implant after exposure to a low-oxygen environment at 700°C.

Fig. 11. Weight change data for Fe-25 wt % Cr and Fe-25 wt % Cr-20 wt % Ni alloys with and without Nb implant after exposure to a low-sulfur mixed-gas environment at 700°C.

Fig. 12. SEM micrographs of surfaces of Fe-25 wt % Cr and Fe-25 wt % Cr-20 wt % Ni alloys with and without Nb implant after exposure to a low-sulfur mixed-gas environment at 700°C.

Fig. 13. SEM micrographs of cross sections of Fe-25 wt % Cr and Fe-25 wt % Cr-20 wt % Ni alloys with and without Nb implant after exposure to a low-sulfur mixed-gas environment at 700°C.

Fig. 14. Weight change data for Fe-25 wt % Cr and Fe-25 wt % Cr-20 wt % Ni alloys with and without Nb implant after exposure to a high-sulfur mixed-gas environment at 700°C.

Fig. 15. SEM micrographs of surfaces of Fe-25 wt % Cr and Fe-25 wt % Cr-20 wt % Ni alloys with and without Nb implant after exposure to a high-sulfur mixed-gas environment at 700°C.

Fig. 16. SEM micrographs of cross sections of Fe-25 wt % Cr and Fe-25 wt % Cr-20 wt % Ni alloys with and without Nb implant after exposure to a high-sulfur mixed-gas environment at 700°C.

TABLE I. Chemical Compositions for Base Alloys Used for Nb Implantation

| | C | Mn | Si | P | S | Cr | Ni | Al | Fe |
|---|---|---|---|---|---|---|---|---|---|
| Fe–25Cr | 0.001 | <0.01 | <0.01 | <0.005 | 0.003 | 25.04 | <0.01 | <0.01 | Bal.* |
| Fe–25Cr–20Ni | 0.004 | <0.01 | <0.001 | <0.005 | 0.002 | 24.84 | 19.91 | 0.01 | Bal. |

*Bal. indicates balance.

TABLE II. Calculated Partial Pressures (in atm) of Oxygen and Sulfur in Various Reaction Gas Mixtures at 700°C

| Gas Mixture | $p_{O_2}$ | $p_{S_2}$ |
|---|---|---|
| Air | 0.21 | – |
| 1 vol. % CO–$CO_2$ | $5.45 \times 10^{-18}$ | – |
| Low–$p_{S_2}$ Gas | $1.91 \times 10^{-21}$ | $3.1 \times 10^{-10}$ |
| High–$p_{S_2}$ Gas | $1.93 \times 10^{-21}$ | $2.5 \times 10^{-8}$ |

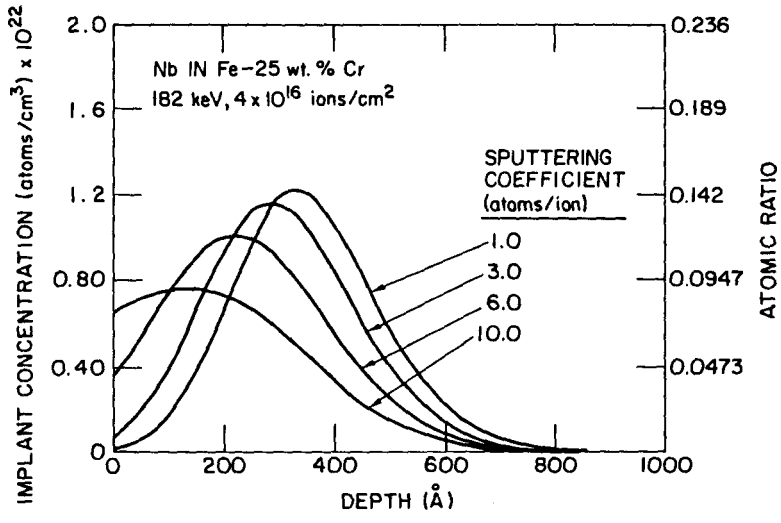
Nb IN Fe-25 wt. % Cr
182 keV, 4 x 10^16 ions/cm^2
SPUTTERING
COEFFICIENT
(atoms/ion)
1.0
3.0
6.0
10.0
IMPLANT CONCENTRATION (atoms/cm^3) x 10^22
ATOMIC RATIO
DEPTH (Å)
2.0
1.6
1.2
0.80
0.40
0
0.236
0.189
0.142
0.0947
0.0473
0
200
400
600
800
1000

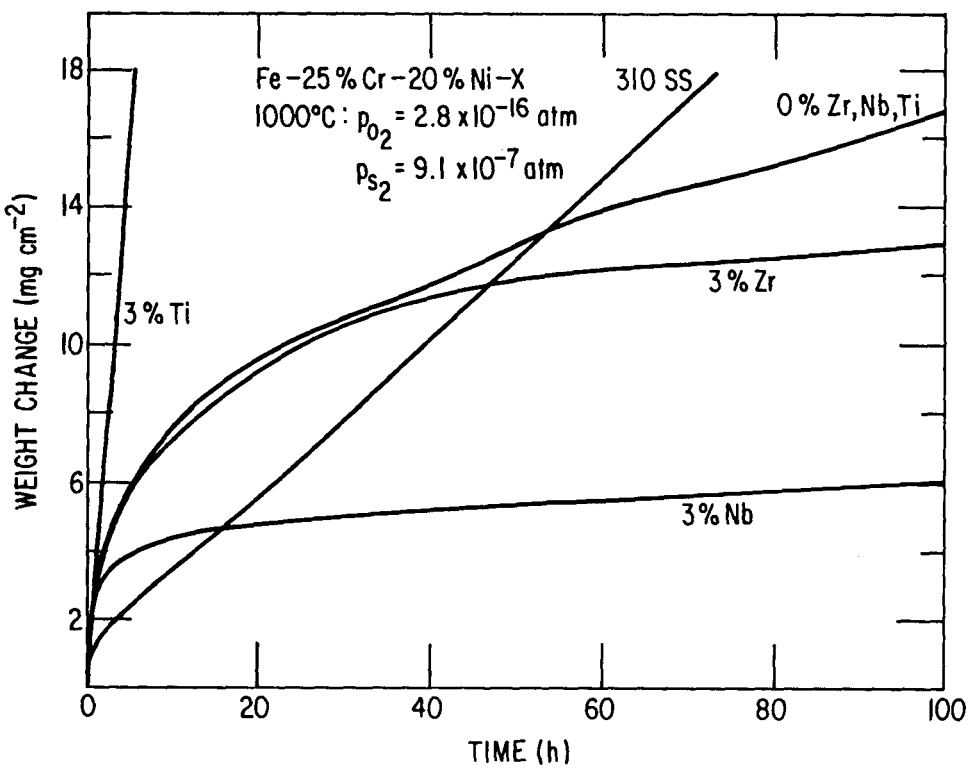
Fe–25% Cr–20% Ni–X
1000°C : $p_{O_2}$ = 2.8 x 10$^{-16}$ atm
$p_{S_2}$ = 9.1 x 10$^{-7}$ atm
310 SS
0% Zr, Nb, Ti
3% Zr
3% Ti
3% Nb
WEIGHT CHANGE (mg cm$^{-2}$)
TIME (h)
0
20
40
60
80
100
2
6
10
14
18

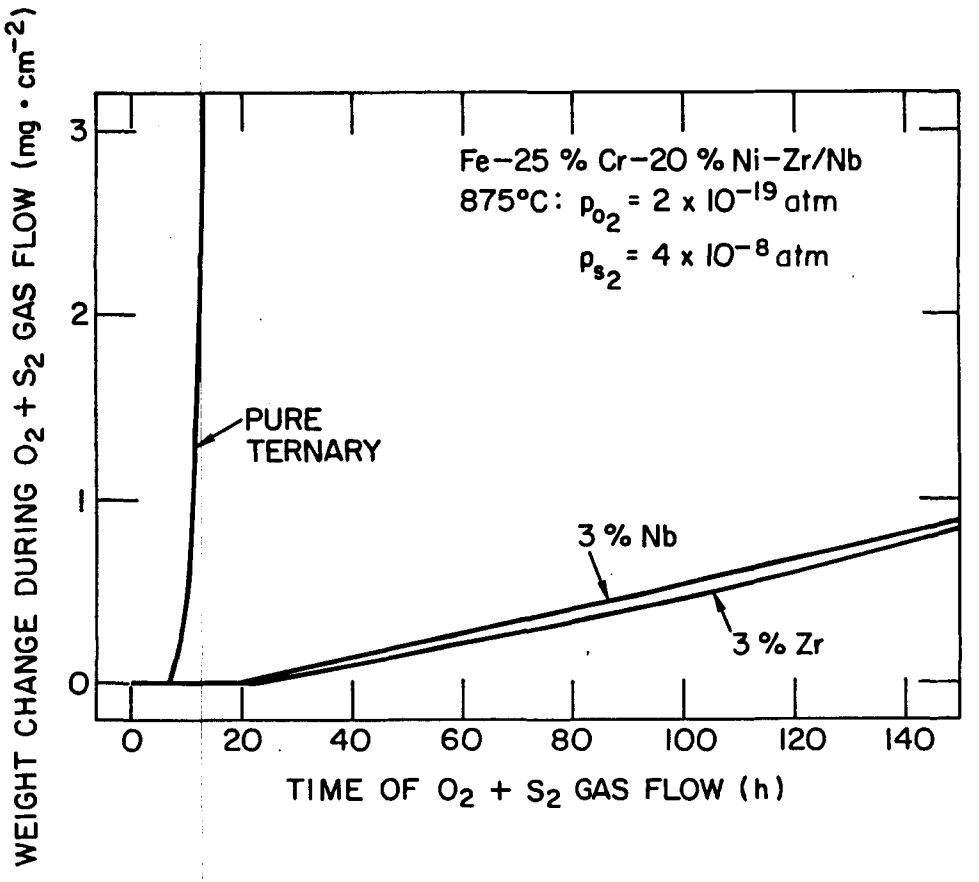
Fe–25 % Cr–20 % Ni–Zr/Nb
875°C: $p_{O_2}$ = 2 x $10^{-19}$ atm
$p_{S_2}$ = 4 x $10^{-8}$ atm
PURE TERNARY
3 % Nb
3 % Zr
WEIGHT CHANGE DURING $O_2$ + $S_2$ GAS FLOW (mg • $cm^{-2}$)
TIME OF $O_2$ + $S_2$ GAS FLOW (h)
0
1
2
3
0
20
40
60
80
100
120
140

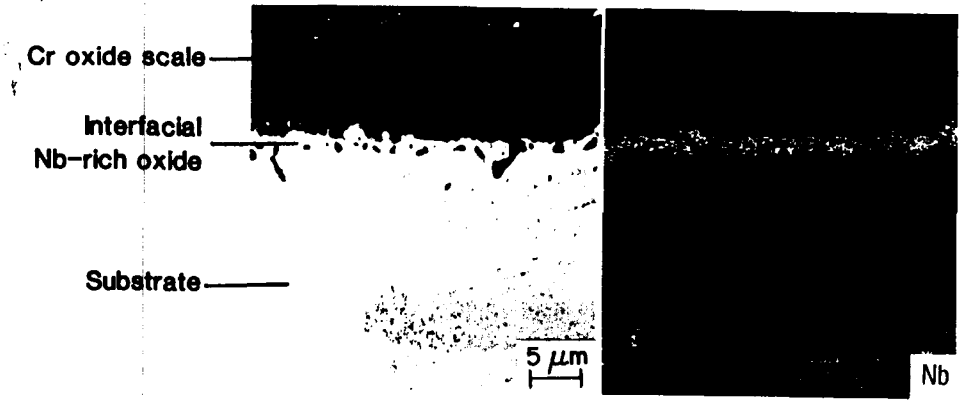
Cr oxide scale
Interfacial
Nb-rich oxide
Substrate
5 μm
Nb

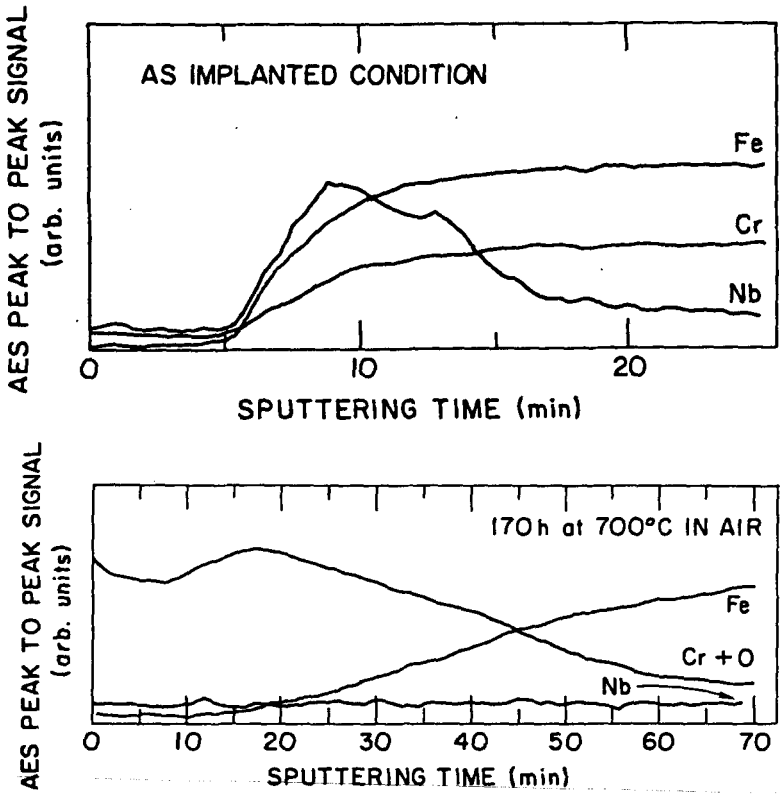
AS IMPLANTED CONDITION
Fe
Cr
Nb
AES PEAK TO PEAK SIGNAL (arb. units)
0
10
20
SPUTTERING TIME (min)
170 h at 700°C IN AIR
Fe
Cr + O
Nb
AES PEAK TO PEAK SIGNAL (arb. units)
0
10
20
30
40
50
60
70
SPUTTERING TIME (min)

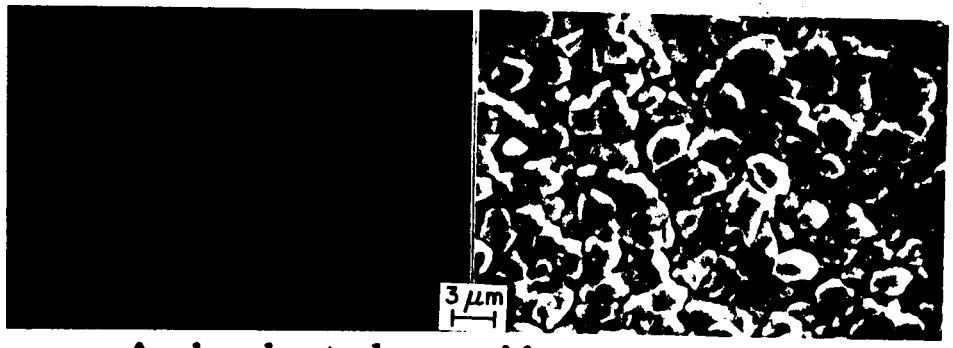


As implanted Air exposed for 170 h

Fe-25Cr

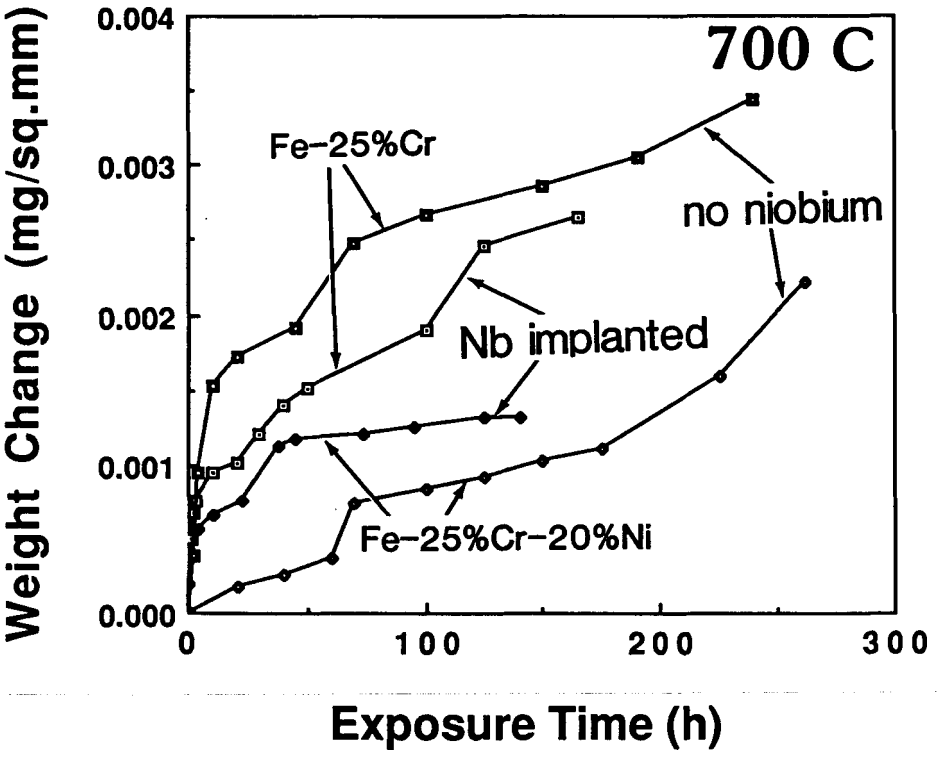
700 C
Fe-25%Cr
no niobium
Nb implanted
Fe-25%Cr-20%Ni
Weight Change (mg/sq.mm)
0.004
0.003
0.002
0.001
0.000
0
100
200
300
Exposure Time (h)

**Air Exposed**

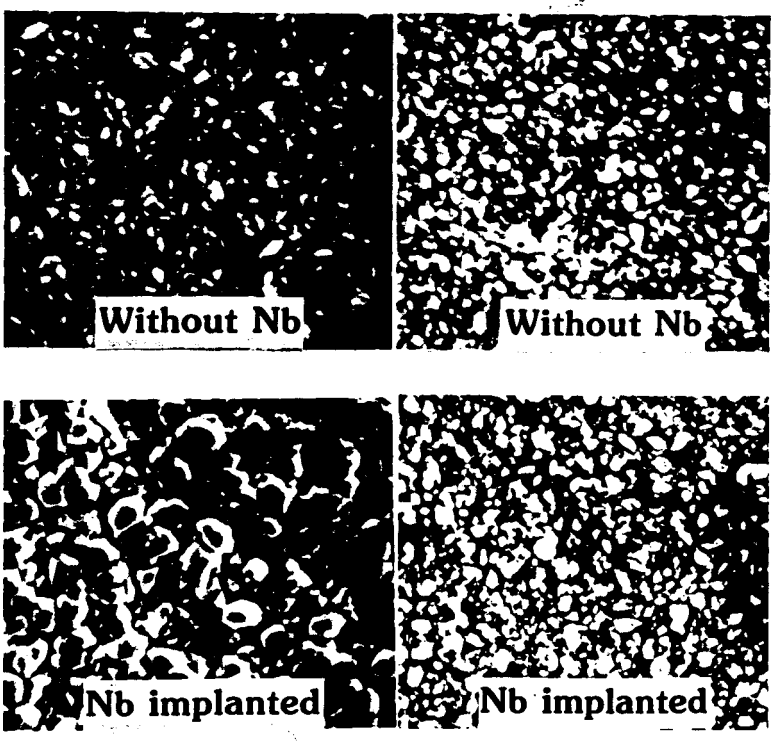


Air Exposed at 700 C

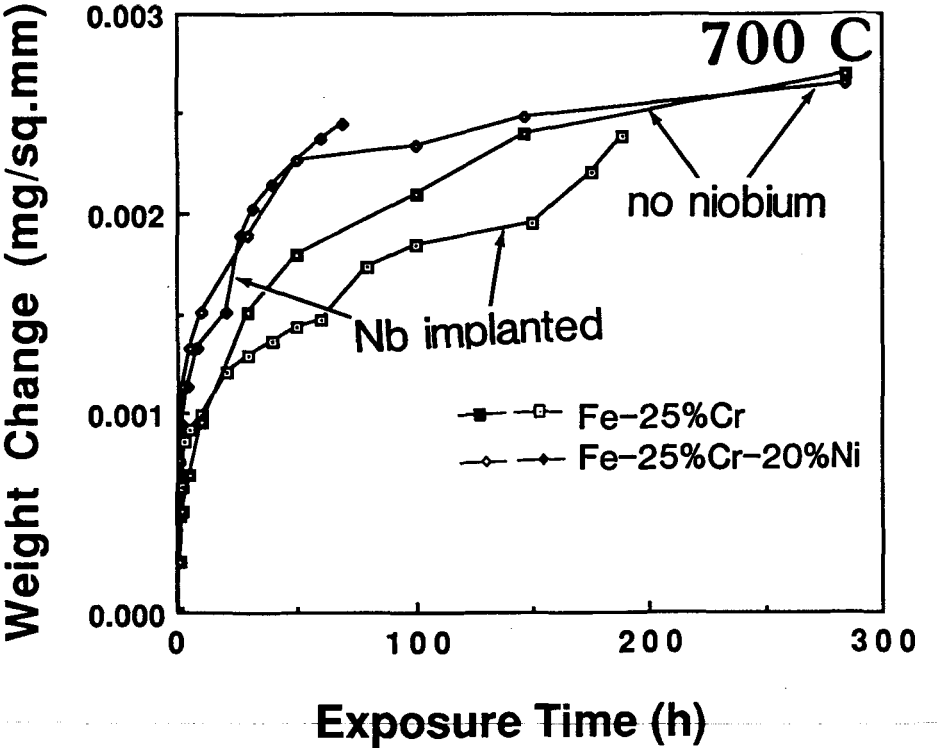


# Low Oxygen Gas

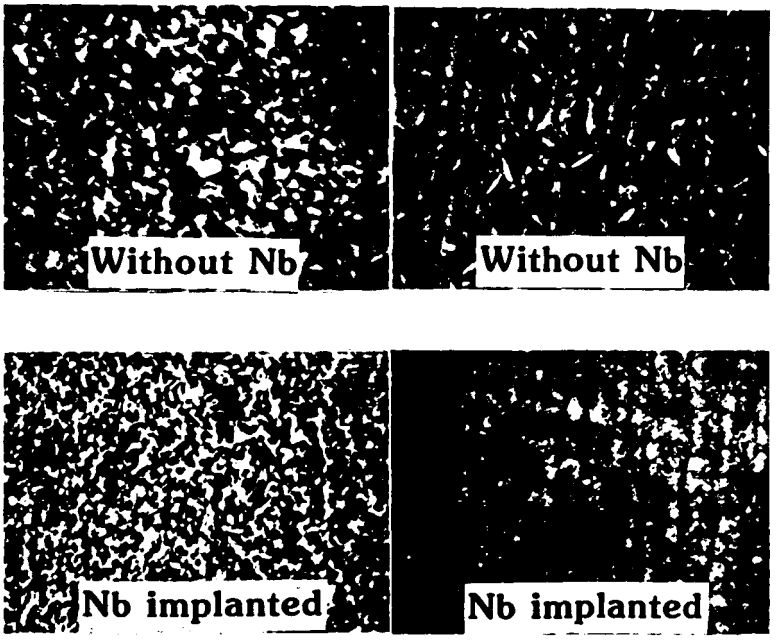


**Exposed to low oxygen gas at 700 C**

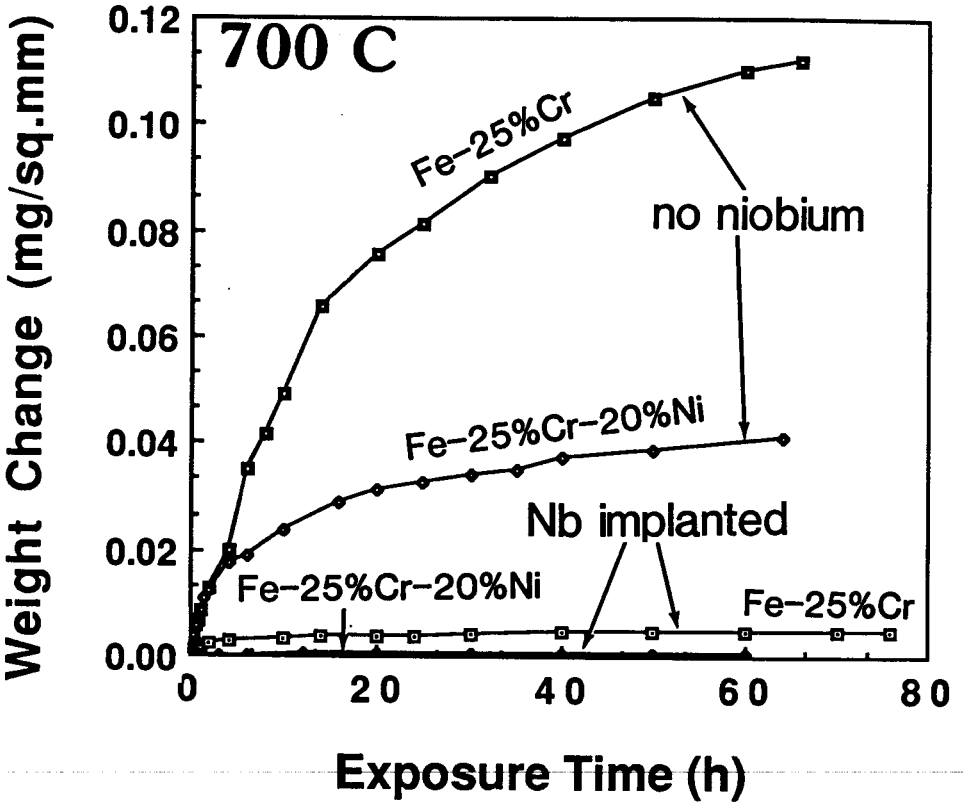


# Low Sulfur Mixed Gas

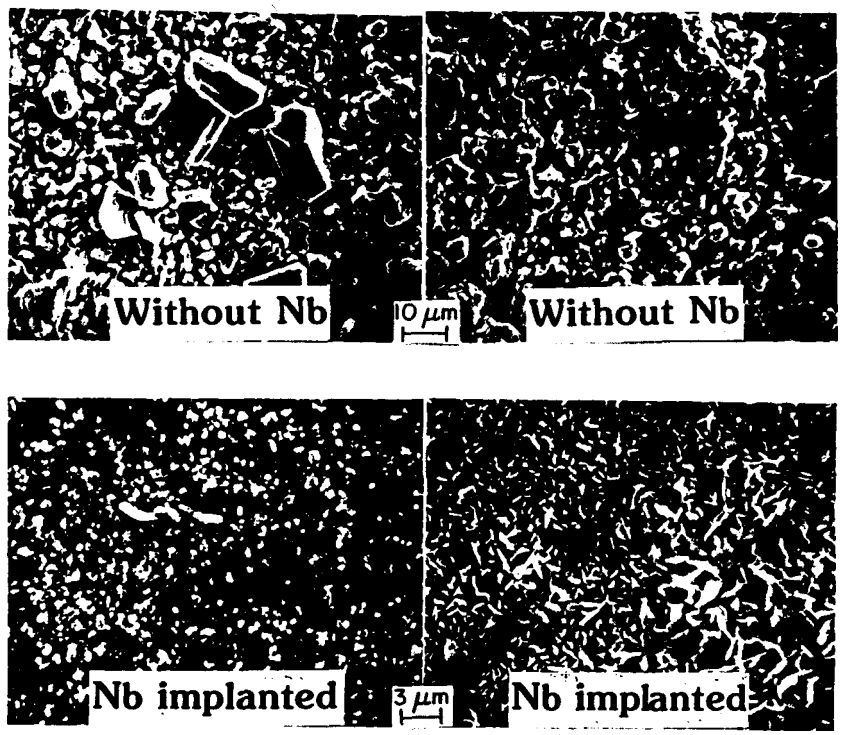


Fe-25Cr Fe-25Cr-20Ni

Low sulfur mixed gas

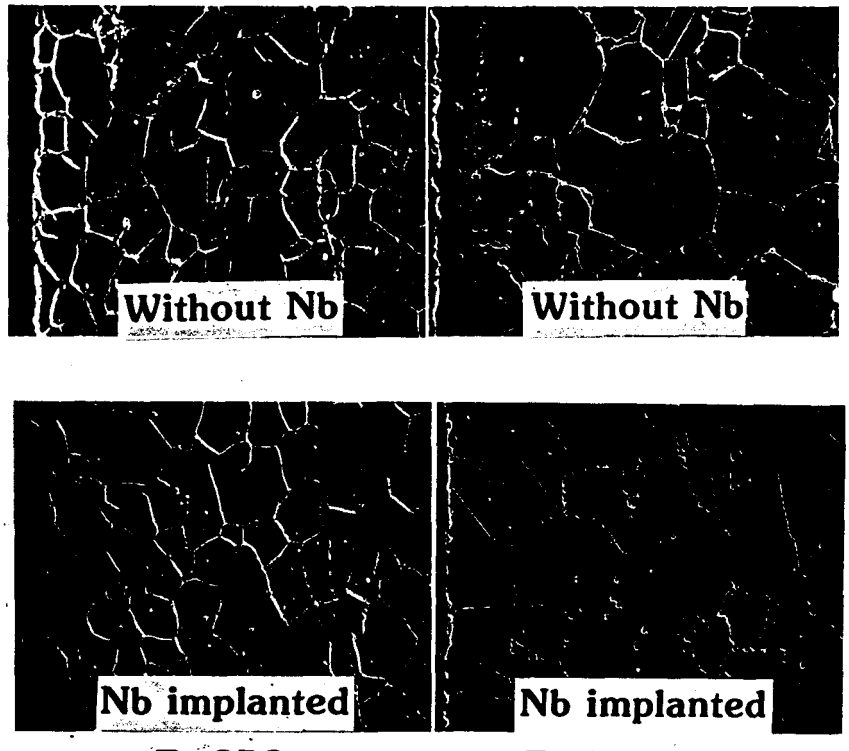


Low sulfur mixed gas

25 μm

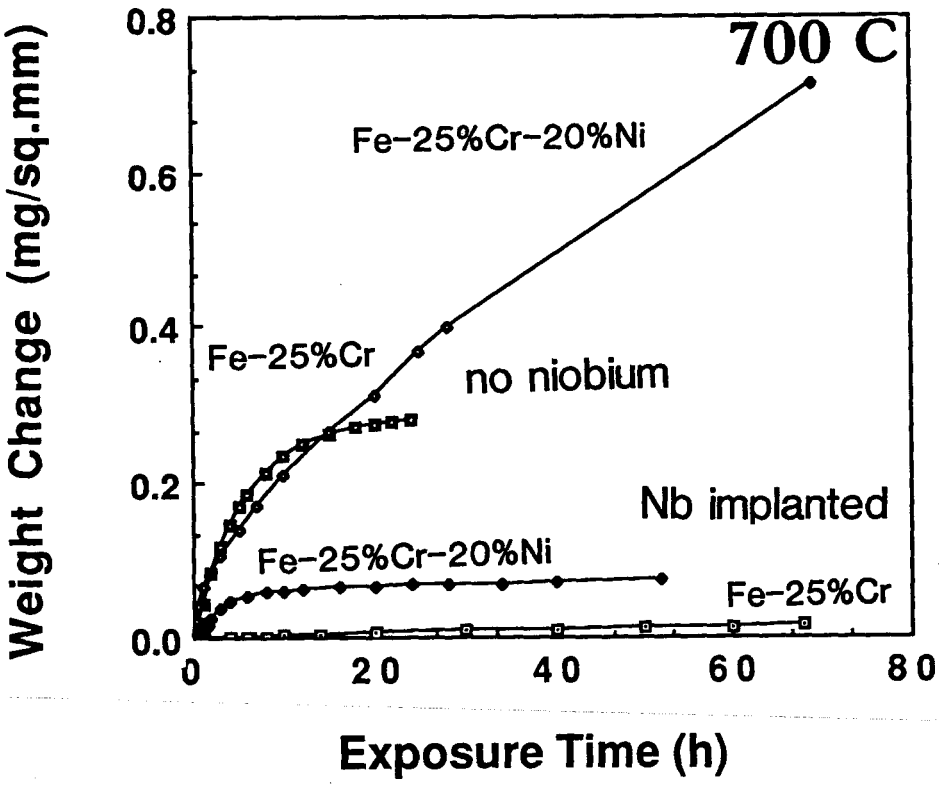


# High Sulfur Mixed Gas

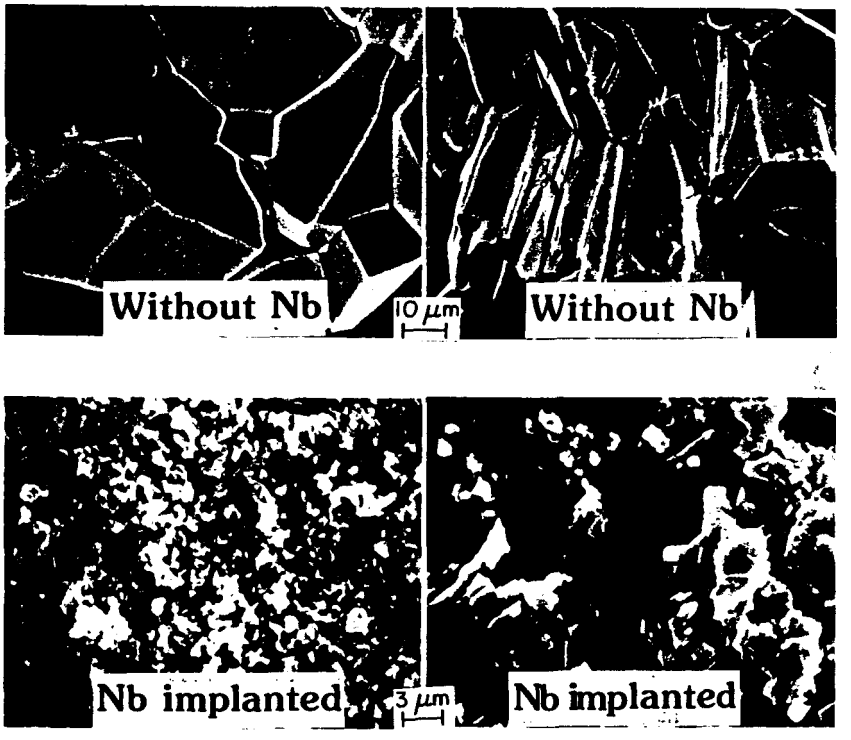


Fe-25Cr Fe-25Cr-20Ni

High sulfur mixed gas

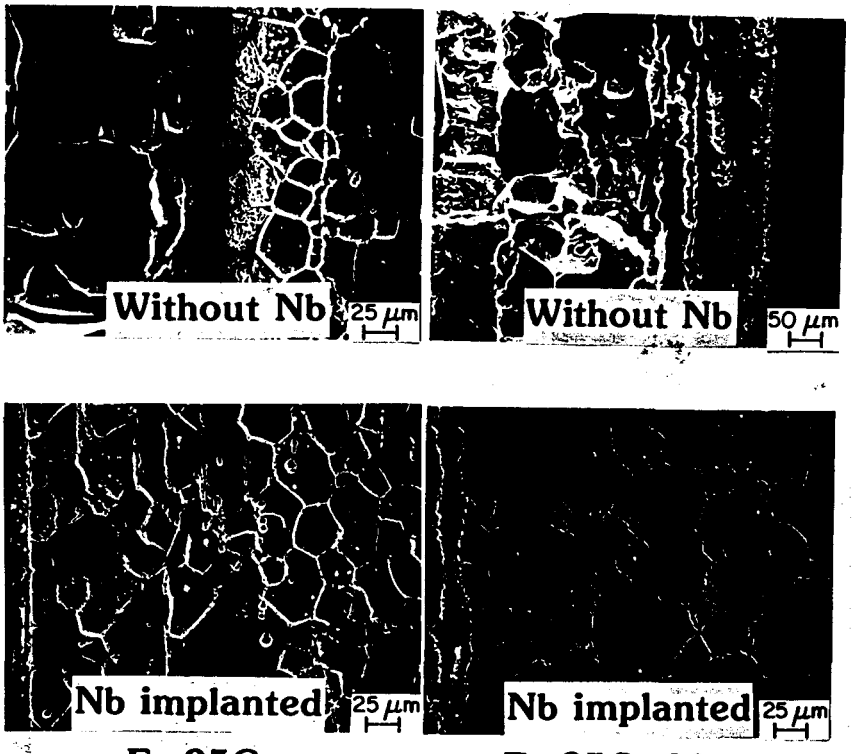


Fe-25Cr Fe-25Cr-20Ni

**High sulfur mixed gas**